

## Wide-band EPR spectroscopy of $\text{SrY}_2\text{O}_4:\text{Ho}^{3+}$ crystal

© G.S. Shakurov<sup>1</sup>, B.Z. Malkin<sup>2</sup>, R.G. Batulin<sup>2</sup>, A.G. Kiiamov<sup>2</sup>

<sup>1</sup>Zavoisky Physical-Technical Institute, FRC Kazan Scientific Center of RAS, Kazan, Russia,

<sup>2</sup>Kazan Federal University, 420008 Kazan, Russia

e-mail:shakurov@kfti.knc.ru

Received July 16, 2021

Revised July 16, 2021

Accepted July 30, 2021

EPR spectra of impurity  $\text{Ho}^{3+}$  ions in oriented  $\text{SrY}_2\text{O}_4$  single-crystals are registered at the temperature 4.2 K in the frequency range from 70 to 180 GHz. The results of measurements evidence for the substitution of  $\text{Ho}^{3+}$  ions for the  $\text{Y}^{3+}$  ions at the structurally nonequivalent sites  $R1$  and  $R2$  with the local  $C_s$  point symmetry. The values of  $g$ -factors, hyperfine structure constants and the energy gaps between the ground and the first excited non-degenerate crystal-field sublevels of the ground  $^5I_8$  multiplet are determined. The observed specific features of the ground states of  $\text{Ho}^{3+}$  ions (non-Kramers doublets with the zero-field splittings of 4.30 and 1.67  $\text{cm}^{-1}$ ) open a possibility to identify transitions in optical spectra of  $\text{SrY}_2\text{O}_4:\text{Ho}$  and inelastic neutron scattering spectra of  $\text{SrHo}_2\text{O}_4$  crystals.

**Keywords:** hyperfine interaction, rare-earth ions, spin Hamiltonian, non-Kramers doublet.

DOI: 10.21883/EOS.2022.01.52983.24-21

### Introduction

EPR spectroscopy of  $\text{Ho}^{3+}$  ions in crystals is presented in a relatively small number of papers, since in a crystal field the ground state of  $\text{Ho}^{3+}$  ion with the electronic configuration  $4f^{10}$  (non-Kramers ion) often turns out to be non-degenerate, and the excitation energy of the state closest to the ground state, as a rule, exceeds the quanta of commercially available spectrometers. At the same time, if the EPR spectra of the  $\text{Ho}^{3+}$  ion can be recorded, then their identification does not cause difficulties when observing the characteristic hyperfine structure (HFS), which consists of eight lines with a large HFS constant. In optical spectra, the resolved HFS of  $\text{Ho}^{3+}$  ion at  $^5I_8 \leftrightarrow ^5I_{7,6}$  transitions was first observed by M.N. Popova et al. [1]. From measurements of high-resolution optical spectra, M.N. Popova discovered and studied additional isotopic structure due to isotopic disorder in the lithium sublattice containing  $^6\text{Li}$  and  $^7\text{Li}$  isotopes in  $\text{LiYF}_4:\text{Ho}^{3+}$  crystal [2]. Later, the spectral isotope effects in the  $\text{LiYF}_4:\text{Ho}^{3+}$  crystal were studied by broadband EPR spectroscopy in the paper [3]. Joint researches with M.N. Popova for the hyperfine interactions in  $\text{KY}_3\text{F}_{10}:\text{Ho}^{3+}$  crystal, effects caused by random deformations in  $\text{CaWO}_4:\text{Ho}^{3+}$  crystal and anticrossings of electron-nuclear levels in  $\text{LiYF}_4:\text{Ho}^{3+}$  and  $\text{CaWO}_4:\text{Ho}^{3+}$  crystals showed that wideband EPR spectroscopy successfully complements high-resolution optical spectroscopy [3–6]. Besides, a large set of experimental data obtained in joint studies made it possible to go beyond the phenomenological description of EPR spectra using the effective spin Hamiltonian. The data analysis of spectroscopic studies based on the Hamiltonian, which operates in the extended space of state of a paramagnetic ion and includes interactions of various physical nature, made it possible to

obtain the parameters characterizing these interactions (in particular, the parameters of crystal fields and exchange interactions). Thus, noting the significant contribution made by M.N. Popova group to the spectroscopy of holmium ions in crystals, we emphasize that cooperation with the Institute of Spectroscopy of the Russian Academy of Sciences made it possible to qualitatively raise the level of researches of EPR spectra at the Kazan Federal University and the Kazan Physical-Technical Institute.

This paper is devoted to wideband EPR spectroscopy of  $\text{SrY}_2\text{O}_4:\text{Ho}^{3+}$  crystal. This compound belongs to the family of oxides of strontium (barium) — rare earths of different composition, but having an identical quasi-one-dimensional crystal structure. Oxides  $\text{SrR}_2\text{O}_4$  ( $R = \text{Y}$ , or a rare-earth (RE) ion) have a space symmetry group of  $P_{nam}$ . An orthorhombic crystal lattice with essentially different values of the translation vectors in the  $ab$ -plane and along the  $c$  axis (lattice constants  $a \sim b$  are approximately three times larger than  $c \sim 0.34$  nm) contains four formula units.  $\text{R}^{3+}$  ions are located in two structurally nonequivalent positions, denoted in the literature as  $R1$  and  $R2$ , and form two pairs of zigzag chains containing two pairs of nearest linear chains of ions propagating along the crystallographic axis  $c$  [7]. Both positions inside deformed oxygen octahedrons (Fig. 1) have local symmetry  $C_s$ . Thus, impurity RE ions replacing  $\text{Y}^{3+}$  ions in  $\text{SrY}_2\text{O}_4$  crystal can form two magnetically nonequivalent centers at  $R1$  and  $R2$  positions. The principal directions of  $g$ -tensors of paramagnetic centers in these positions can lie in  $(ab)$  plane or are parallel to the  $c$  axis.  $\text{SrY}_2\text{O}_4$  crystals activated by erbium ions were studied earlier by the EPR method in the paper [8], and a strong anisotropy of  $g$ -tensors of  $\text{Er}^{3+}$  ions was found both in positions  $R1$  and  $R2$ . As was shown in [8], the nature of the anisotropy (the relative value of the axial (along  $c$  axis)

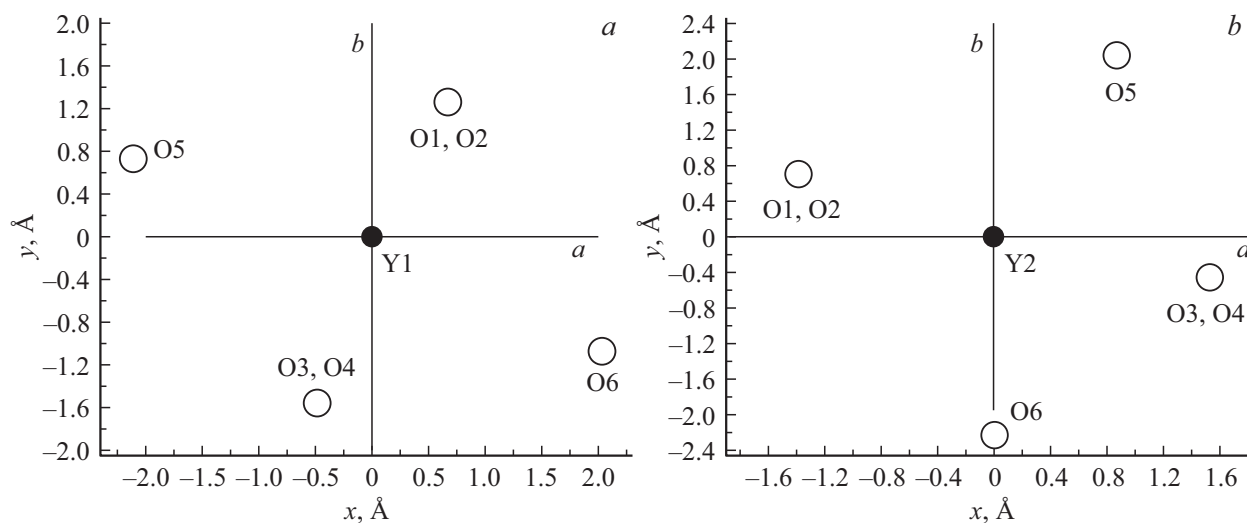


**Figure 1.** Projections of oxygen ions from the nearest environment of yttrium ions in positions (a)  $R1$  and (b)  $R2$  onto the reflection plane ( $ab$ ). The ion coordinates along  $c$  axis are  $c/2$  (O1, O3),  $-c/2$  (O2, O4) and zero (O5, O6),  $c$  is the lattice constant.

component and the transversal components of  $g$ -tensor (in  $ab$  plane) is determined by the ratio of the parameters of the axial and rhombic components of the crystal field, i.e., mainly by the distortion characteristics of the oxygen octahedrons surrounding the RE ion. In particular, since the oxygen octahedra in the  $R2$  positions are characterized by strong stretching in the direction parallel to ( $ab$ ) plane, the ratio of the largest  $g$ -factor in the plane to the axial component for  $\text{Er}^{3+}$  ions ( $R2$ ), which is 3.86, is much larger than this ratio, equal to 0.54, at the position  $R1$  [8].

Magnetic and spectral properties of magnetically concentrated RE oxides  $\text{SrR}_2\text{O}_4$ ,  $\text{BaR}_2\text{O}_4$ , which are geometrically frustrated magnets with competing magnetic interactions between RE ions in zigzag chains have been intensively studied over the past 15 years [7,9–11]. Nevertheless, the problems associated with the identification of the electronic structure of RE ions in structurally nonequivalent positions and the formation of ordered magnetic structures remain relevant at the present time.

## Experiments and measurement results

Two single crystals with holmium concentrations of 2.5 at.% and 0.25 at.% were studied. Sample  $\text{SrY}_2\text{O}_4:\text{Ho}^{3+}$  (2.5 at.%) was grown at the University of Warwick (England), the second crystal was grown at Kazan Federal University. The technique for growing  $\text{SrR}_2\text{O}_4$  oxides is described in papers [8,12]. The samples were oriented using an X-ray diffractometer.

The EPR spectra were obtained using wideband spectrometer at liquid helium temperatures in magnetic fields up to 1 T [13]. The measurements were made for collinear mutual polarization of constant and alternating magnetic fields ( $\mathbf{B} \parallel \mathbf{B}_1$ ). Two crystallographically different centers of  $\text{Ho}^{3+}$  ion were found.

The EPR signals of Ho1 centers assigned to the  $R1$  position on the basis of the found for these centers easy-axis magnetic anisotropy in the direction of  $c$  axis were observed at the magnetic field orientation  $\mathbf{B} \parallel c$ . The measured spectra are shown in Fig. 2, and the frequency vs. field diagrams of resonant transitions are shown in Fig. 3. The EPR lines of the second Ho2 center were observed in the frequency range of 70–150 GHz in magnetic fields  $\mathbf{B} \perp c$ ; they have a resolved HFS for both samples with different concentrations of impurity ions and differ from the Ho1 spectra by the presence of two spectra, corresponding to two magnetically nonequivalent  $R2$  positions of holmium ions in the unit cell of the crystal lattice. Figure 4 shows the EPR spectra of Ho2 centers at frequencies 98 and 112.4 GHz, when two magnetically-conjugated spectra are merged (in the magnetic fields  $\mathbf{B} \parallel b$ ). For the  $\mathbf{B} \parallel b$  orientation, a frequency vs. field dependence was plotted (Fig. 5), the comparison of which with the corresponding dependence for Ho1 centers (Fig. 3) shows a significant difference (approximately by two times) in the energy intervals between the ground and first excited states of holmium ions in crystal fields in the Ho1 and Ho2 centers.

It can be concluded from Figs. 3 and 5 that the observed EPR spectra for Ho1 and Ho2 centers are due to resonant transitions between the ground and first excited singlets (sublevels of the ground multiplet of holmium ions  $^5I_8$ , completely split in a low-symmetry crystal field). Since no other excited levels of holmium ions were detected up to 630 GHz, the resonant transitions take place between sublevels of isolated non-Kramers quasi-doublets. In this case, there is only one nonzero component of the magnetic dipole moment of Ho1 centers, directed along the  $c$  axis [14]. A feature of the EPR spectra of the Ho1 center was the presence of a large number of satellites both near the basic HFS lines and overlapping with them (Fig. 2) in a sample with a concentration of 2.5 at.%. The

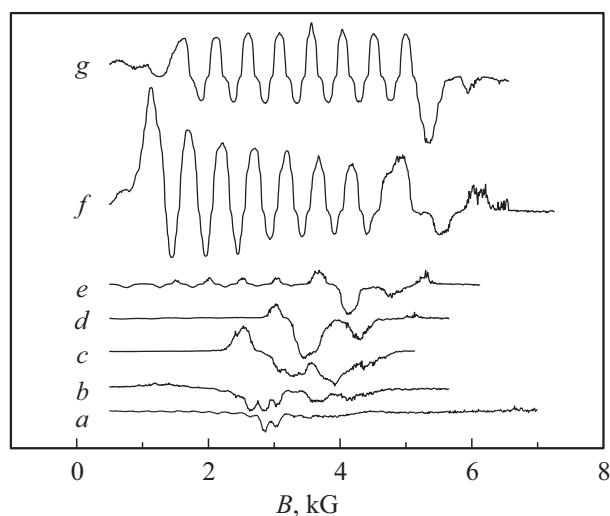


**Figure 2.** View of the EPR spectra in  $\text{SrY}_2\text{O}_4:\text{Ho}^{3+}$  (2.5 at.%) crystal for  $\mathbf{B} \parallel c$  orientation. Frequencies: *a* — 122 GHz, *b* — 126 GHz, *c* — 129 GHz, *d* — 132 GHz, *e* — 135 GHz, *f* — 144 GHz, *g* — 150 GHz.

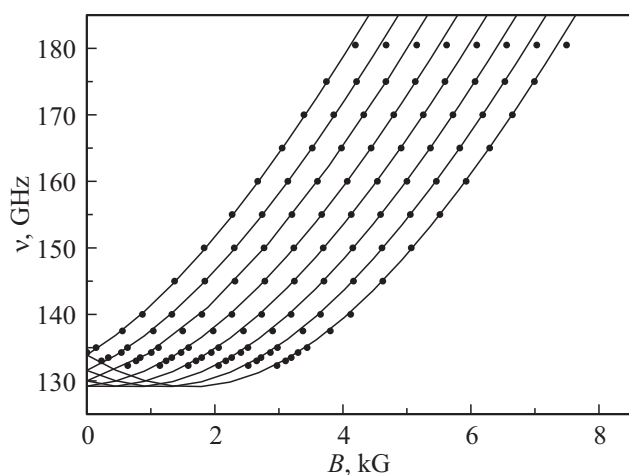


**Figure 3.** Frequency vs. field of resonant transitions of  $\text{Ho}^{3+}$  ions in  $\text{SrY}_2\text{O}_4$  crystal (Ho1 centers). Orientation  $\mathbf{B} \parallel c$ . Symbols — measurement data, lines — calculation results (see equation (3)).

presence of other types of single centers, caused by a slight change in the crystal field, seems unlikely, since the  $\text{Ho}^{3+} \leftrightarrow \text{Y}^{3+}$  substitution is isovalent. We can make a preliminary conclusion that when  $\text{Y}^{3+}$  ions are replaced by  $\text{Ho}^{3+}$  ions in the *R1* position, in addition to single centers the pair centers with weak interaction between ions are formed. The relatively weak interaction is shown by the fact that the satellites are located inside HFS of the main signals and have close values of the initial splittings of the quasi-doublets. In particular, at frequencies of 146 and 150 GHz, the satellites are clearly visible on the low-field line of the hyperfine structure, and are also superimposed on the lines of the basic spectrum (Fig. 2). At frequencies below 132 GHz, where the spectrum of a single  $\text{Ho}^{3+}$  ion is

no longer visible (Fig. 2), high-field satellites continue to be detected. In a zero magnetic field, the minimum excitation energy of pair centers is about 120 GHz. The possibility of observing EPR signals of pair centers of  $\text{Ho}^{3+}$  ions in the *R1* positions with magnetic moments along *c* axis is due to the specific quasi-one-dimensional structure of  $\text{SrY}_2\text{O}_4$  crystal lattice, in which zigzag chains of  $\text{Y}^{3+}$  ions are formed by two close linear chains propagating along the *c* axis and shifted relative to each other by half of the lattice constant along this axis. In Ho1-Ho1 pair centers, formed by two close ions in the linear chain, the magnetic moments are parallel to the vector connecting the ions. In this case the dipole-dipole interaction has a maximum value and leads to registered changes in the spectrum of single centers, while in Ho2-Ho2 pair centers with magnetic moments in *ab*-

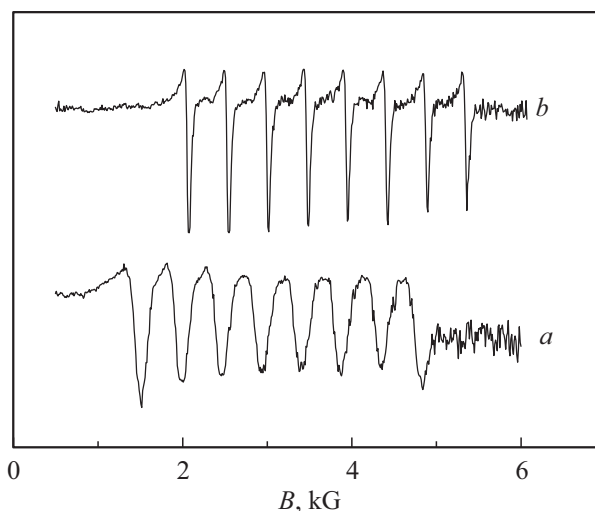


**Figure 4.** View of EPR spectra in crystal *a* —  $\text{SrY}_2\text{O}_4:\text{Ho}^{3+}$  (2.5 at.%), frequency 98 GHz, *b* —  $\text{SrY}_2\text{O}_4:\text{Ho}^{3+}$  (0.25 at.%), frequency 112.4 GHz. Orientation  $\mathbf{B} \parallel b$ .

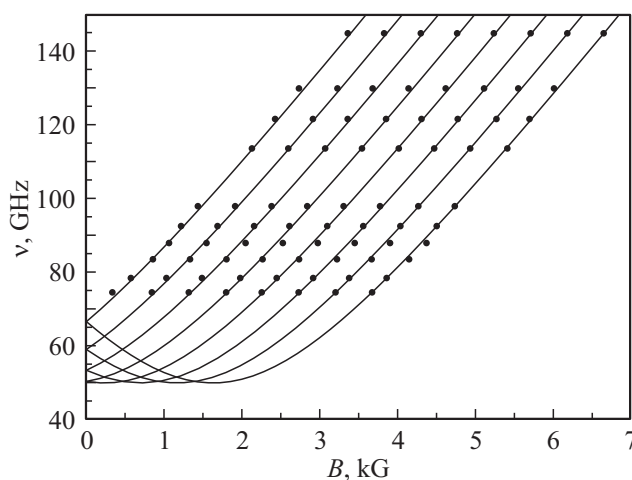


**Figure 5.** Frequency vs. field of resonant transitions of  $\text{Ho}^{3+}$  ions in  $\text{SrY}_2\text{O}_4$  crystal (Ho2 centers). Orientation  $\mathbf{B} \parallel b$ . Symbols — experiment, lines — calculation results in accordance with equation (4).

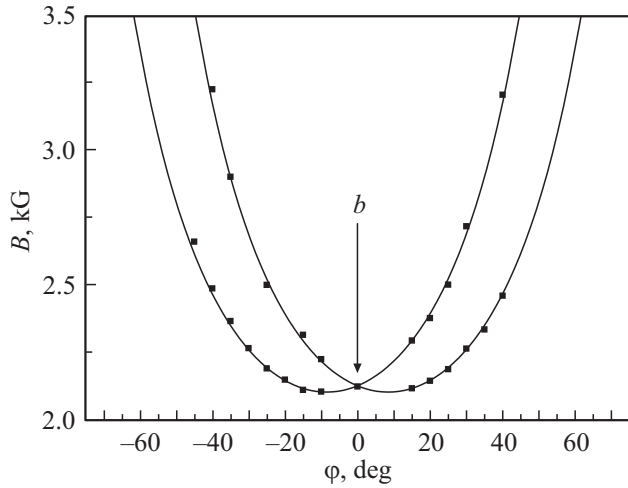


**Figure 6.** Angular dependence of the resonant magnetic field in  $(ab)$  plane at frequency of 113.7 GHz for the low-field hyperfine component of the EPR signals of  $\text{Ho}^{3+}$  ions at Ho2 centers in crystal  $\text{SrY}_2\text{O}_4:\text{Ho}^{3+}$  (2.5 at.%). Symbols — experiment, lines — approximation by function  $B(\varphi) = B(\varphi_0)/\cos(\varphi \pm \varphi_0)$ , where  $\varphi_0 = 8.5^\circ$ .

plane, the dipole-dipole interaction is much weaker, and the registration of satellites, which do not go beyond the width of the lines of single centers, is impossible.

Angular diagrams of the EPR spectra of  $\text{Ho}^{3+}$  ions in two magnetically nonequivalent positions Ho2 under the magnetic field  $\mathbf{B}$  rotation in  $(ab)$  plane are shown in Fig. 6. For clarity, the graph shows the dependence of only the low-field HFS component. The angle of direction deviation of the field corresponding to the maximum  $g$ -factor from the crystallographic axis  $b$  was  $\sim 8.5$  degrees. Under rotation in the  $(bc)$  plane, the lines of two magnetically nonequivalent centers were merged.

## Discussion of results

Neglecting the nuclear Zeeman energy in the external magnetic field  $\mathbf{B}$ , the energy of the nuclear quadrupole moment of holmium ions, and mixing the wave functions of the sublevels of the basic quasi-doublet with the wave functions of the excited sublevels of the multiplet  $^5I_8$ , we analyzed the measurement results using the method of effective spin Hamiltonian [14]. In the calculations of the frequency versus field dependences, the following spin Hamiltonians (effective spin  $S = 1/2$ ) were used, defined in the Cartesian coordinate system ( $z \parallel c$ ) in the space of electron-nuclear states corresponding to the electronic quasi-doublet and the nuclear spin  $I = 7/2$ ,

$$H_{S,\text{Ho1}} = \Delta_1 S_y + (A_1 I_z + g_1 \mu_B B_z) S_z \quad (1)$$

for  $\text{Ho}^{3+}$  ions in Ho1 centers, and

$$H_{S,\text{Ho2}} = \Delta_2 S_{x'} + [A_2 I_{y'} + g_2 \mu_B B_\perp \cos(\varphi \mp \varphi_0)] S_{y'}, \quad (2)$$

for  $\text{Ho}^{3+}$  ions in Ho2 centers, where  $S_\alpha$  are the effective spin components,  $\varphi$  is the angle between the field  $\mathbf{B}_\perp$  perpendicular to  $c$  axis and the  $b$  axis,  $y'$  axes lie in  $(ab)$  plane and are the principal directions of the corresponding  $g$ -tensors (the corresponding principal value is  $g_2$ ) for two magnetically nonequivalent Ho2 centers deviated from the  $b$  axis by an angle  $\pm \varphi_0$ . The dependences of resonant frequencies  $\nu$  versus magnetic field parallel to  $c$  axis for holmium ions in positions Ho1, or parallel to  $b$  axis for holmium ions in positions Ho2, are determined by the expressions

$$2\pi\hbar\nu = [\Delta_1^2 + (A_1 m + g_1 \mu_B B_c)^2]^{1/2} \quad (3)$$

and

$$2\pi\hbar\nu = \{\Delta_2^2 + [A_2 m' + g_2 \mu_B B_\perp \cos(\varphi)]^2\}^{1/2} \quad (4)$$

for Ho1 and Ho2 centers, respectively, where  $m$  and  $m'$  determine the projections of the nuclear spin ( $\pm 1/2, \pm 3/2, \pm 5/2, \pm 7/2$ ) onto the direction of the electronic magnetic moment of the corresponding center. The value of the angle  $\varphi_0 = 8.5^\circ$  was found from the measurement results of resonant magnetic fields in  $ab$ -plane at a fixed frequency  $\nu$  of the alternating magnetic field dependences on the angle  $\varphi$  (Fig. 6), which were reproduced with good accuracy by the function

$$B(\varphi) = \{[(2\pi\hbar\nu)^2 - \Delta_2^2]^{0.5} - A_2 m'\} / g_2 \mu_B \cos(\varphi \pm \varphi_0). \quad (5)$$

The values, obtained as result of simulations of frequency vs. field dependences, of initial splittings of quasi-doublets  $\Delta_1, \Delta_2$ ,  $g$ -factors  $g_1, g_2$  and hyperfine interaction constants  $A_1$  and  $A_2$  for holmium ions in the Ho1 and Ho2 centers are for Ho1:  $\Delta_1 = 129.1 \text{ GHz} = 4.303 \text{ cm}^{-1}$ ,  $g_1 = 15.71$ ,  $A_1 = 10.15 \text{ GHz} = 0.338 \text{ cm}^{-1}$ ; for Ho2:  $\Delta_2 = 50 \text{ GHz} = 1.667 \text{ cm}^{-1}$ ,  $g_2 = 19.31$ ,  $A_2 = 12.6 \text{ GHz} = 0.42 \text{ cm}^{-1}$ .

Calculation results of resonant magnetic fields in accordance with expressions (3), (4), represented by solid lines in Figs. 3 and 5, are in good agreement with the measurement data. Note that found in this paper  $g$ -factors and orientations of the magnetic moments of  $\text{Ho}^{3+}$  ions in the  $R1$  and  $R2$  positions along  $c$  and  $b$  crystallographic axes, respectively, agree qualitatively with results previously obtained from the analysis of the spectra of inelastic neutron scattering in  $\text{SrHo}_2\text{O}_4$  isostructural crystal in [11].

## Conclusion

The main result of the measurements of the EPR spectra of oriented  $\text{SrY}_2\text{O}_4:\text{Ho}^{3+}$  single crystals presented in this paper is the determination of the spectral and magnetic characteristics of  $\text{Ho}^{3+}$  impurity ions substituting for  $\text{Y}^{3+}$  ions in two structurally nonequivalent positions with the same local symmetry  $C_s$ , but significantly different in the degree of deformation of the oxygen octahedrons surrounding the trivalent cations. The found values of the initial

splittings and  $g$ -factors for the ground non-Kramers quasi-doublets can be directly compared with the data obtained by magnetometry, optical and neutron spectroscopy in diluted and concentrated Sr(Y<sub>1-x</sub>Ho<sub>x</sub>)<sub>2</sub>O<sub>4</sub> crystals, and serve as the basis for the development of the microscopic theory of singlet magnetism in these frustrated magnets.

### Acknowledgments

Authors are grateful to O.A. Petrenko for oriented sample SrY<sub>1.95</sub>Ho<sub>0.05</sub>O<sub>4</sub> provided for EPR spectra measurements.

### Funding

The work of G.S.Sh. (measurement of EPR spectra) was carried out under the government assignment for FRC Kazan Scientific Center of RAS, the work of B.Z.M., R.G.B. and A.G.K. at KFU (growing and orienting SrY<sub>2</sub>O<sub>4</sub>:Ho<sup>3+</sup> single crystals, analysis of measurement results) was supported by the Russian Science Foundation (project № 19-12-00244).

### Conflict of interest

The authors declare that they have no conflict of interest.

### References

- [1] N.I. Agladze, M.N. Popova. *Solid State Commun.*, **55** (12), 1097 (1985). DOI: 10.1016/0038-1098(85)90141-3
- [2] N.I. Agladze, M.N. Popova, G.N. Zhizhin, V.J. Egorov, M.A. Petrova. *Phys. Rev. Lett.*, **66** (4), 477 (1991). DOI: 10.1103/PhysRevLett.66.477
- [3] G.S. Shakurov, M.V. Vanyunin, B.Z. Malkin, B. Barbara, R.Yu. Abdulsabirov, S.L. Korableva. *Appl. Magn. Reson.*, **28** (3–4), 251 (2005). DOI: 10.1007/BF03166760
- [4] D.S. Pytalev, E.P. Chukalina, M.N. Popova, G.S. Shakurov, B.Z. Malkin, S.L. Korableva. *Phys. Rev. B.*, **86** (11), 115124 (2012). DOI: 10.1103/PhysRevB.86.115124
- [5] G.S. Shakurov, E.P. Chukalina, M.N. Popova, B.Z. Malkin, A.M. Tkachuk. *Phys. Chem. Chem. Phys.*, **16** (45), 24727 (2014). DOI: 10.1039/C4CP03437F
- [6] K.N. Boldyrev, M.N. Popova, B.Z. Malkin, N.M. Abishev. *Phys. Rev. B.*, **99** (4), 041105 (2019). DOI: 10.1103/PhysRevB.99.041105
- [7] H. Karunadasa, Q. Huang, B.G. Ueland, J.W. Lynn, P. Schiffer, K.A. Regan, R.J. Cava. *Phys. Rev. B.*, **71** (14), 144414 (2005). DOI: 10.1103/PhysRevB.71.144414
- [8] B.Z. Malkin, S.I. Nikitin, I.E. Mumdzhi, D.G. Zverev, R.V. Yusupov, I.F. Gilmutdinov, R.G. Batulin, B.F. Gabbasov, A.G. Kiiamov, D.T. Adroja, O. Young, O.A. Petrenko. *Phys. Rev. B.*, **92** (9), 094415 (2015). DOI: 10.1103/PhysRevB.92.094415
- [9] O.A. Petrenko. *Low Temp. Phys.*, **40** (2), 106 (2014). DOI: 10.1063/1.4865556
- [10] O. Young, G. Balakrishnan, P. Manuel, D.D. Khalyavin, A.R. Wildes, O.A. Petrenko. *Crystals.*, **9** (10), 488 (2019). DOI: 10.3390/cryst9100488
- [11] A. Fennell, V.Y. Pomjakushin, A. Uldry, B. Delley, B. Prevost, A. Desilets-Benoit, A.D. Bianchi, R.I. Bewley, B.R. Hansen, T. Klimczuk, R.J. Cava, M. Kenzelmann. *Phys. Rev. B.*, **89** (22), 224511 (2014). DOI: 10.1103/PhysRevB.89.224511
- [12] G. Balakrishnan, T.J. Hayes, O.A. Petrenko, D.McK. Paul. *J. Phys.: Condens. Matter.*, **21** (1), 012202 (2009). DOI: 10.1088/0953-8984/21/1/012202
- [13] V.F. Tarasov, G.S. Shakurov. *Appl. Magn. Reson.*, **2** (3), 571 (1991). DOI: 10.1007/BF03166064
- [14] J.S. Griffith. *Phys. Rev.*, **132** (1), 316 (1963). DOI: 10.1103/PhysRev.132.316